Barium Cation Complexation by Flexible Mono- and Ditopic Receptors, Studied by UV Absorption and Fluorescence Spectroscopy

Ezequiel Perez-Inestrosa,*[a] Jean-Pierre Desvergne,*[b] Henri Bouas-Laurent,[b] Jean-Claude Rayez,[c] Marie-Thérèse Rayez,[c] Michel Cotrait,[b] and Pierre Marsau[b]

Dedicated to Anne-Marie Albrecht-Gary on the occasion of her 55th birthday

Keywords: Barium / Cooperativity effect / Crown compounds / Luminescence / Transitory photodecomplexation

The metal cation (Ba^{++}) binding ability of a *family* of designed nonconjugated bichromophoric [bis(*para*-phenylene)- or bis(*para*-diphenylene)]polyoxamacrocyclic *coronands* has been studied in acetonitrile in the ground state and in the singlet excited state. The association constants (*K*) at ambient temperature have been determined from UV absorption and fluorescence data, by use of the LETAGROP-SPEFO programme. The ground state complexes exhibit 1:1 or 1:1 and 2:1 (cation/ligand) stoichiometries and a large variety of association constants, as well as diverse cooperative effects. Remarkably, TTO_5O_5 {1,4,7,10,13,21,24,27,30,33-decaoxa-[13.15]-(1,4)benzenophane} shows a strong binding ability ($\log \beta = 10.3$) with a positive cooperativity. The apparent association constants measured from stationary fluorescence data were found to be lower in some cases than those observed in the ground state; these results strongly suggest that a transitory photodecomplexation between the metal cation and the phenolic oxygen atoms occurs in the S_1 state. An X-ray structure analysis was performed on the *barium* complex of a related *podand* and the Ba^{++} coordination number was found to be 10.

1. Introduction

The bichromophoric 34-membered macrocycle (BBO_5O_5) shown in Figure 1 is a *monocyclic* endoreceptor[1] composed of two *rigid* subunits symmetrically incorporated into a ring made up of 8 *flexible* polyoxyethylene (POE) repeating units. This combination of rigidity and flexibility confers particular properties on this *coronand*; these differ from those of the regular Pedersen crown ethers (in which the phenyl rings are *ortho*-disubstituted; see Figure 1).

Thanks to the presence of two electron-rich benzene rings at appropriate positions in the macrocycle, BBO_5O_5 has been shown to form 1:1 charge transfer complexes with molecular dications such as methylviologen (paraquat^{++}).[2]

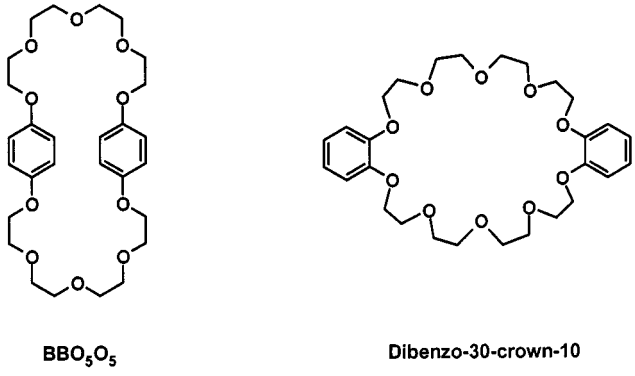

Figure 1. Bis-*p*-phenylene coronand BBO5O5 (B: denotes *p*-benzenediyl), 34-membered macrocycle (10 oxygen atoms); this coronand, unlike dibenzo-30 crown ether, is not a regular crown ether

These complexes are formed with little change in the shape of the molecular receptor, a large cavity (10.6 × 4.7 Å) in the solid state.[2] Moreover, the two aromatic rings of the free coronands can act as *spacers* between two potential hosting sites for metal cations (the so-called "ditopic receptors");[3] the compound has the flexibility necessary to encapsulate either one or two cationic guests, as demonstrated by the formation of 1:1 and 2:1 (cation/ligand) complexes with Na^+, Ca^{++} and Sr^{++}.[3] For the 2:1 complexes, a negative *cooperative* effect was observed and the results of

[a] Departamento de Química Orgánica, Facultad de Ciencias, Universidad de Málaga, Campus Teatinos
29071 Malaga, Spain
Fax: (internat.) + 34-952/131941
E-mail: inestrosa@uma.es
[b] Laboratoire de Chimie Organique et Organométallique, CNRS-UMR 5802, Université Bordeaux 1
33405 Talence Cedex, France
Fax: (internat.) + 33-5/56846646
E-mail: jp.desvergne@lcoo.u-bordeaux.fr
[c] Laboratoire de Physico-Chimie Moléculaire, CNRS-UMR 5803, Université Bordeaux 1
33405 Talence Cedex, France
Fax: (internat.) + 33-5/56846645
E-mail: rayez@cribx1.u-bordeaux.fr

  1434–193X/02/0102–0331 $ 17.50+.50/0

a spectroscopic study suggested that *partial photodecomplexation* occurs in the relaxed excited singlet state.[3a,3b]

This latter observation has analogies in recent findings concerning the photodissociation of 1:1 metal cation complexes of *mono*cyclic receptors incorporating a juxtanuclear amino group[4–6] and some benzocrown ethers,[7] although all these systems, in contrast to BBO_5O_5, are strongly dissymmetrical.

Because of the properties of BBO_5O_5 regarding *photoswitching of metal cation capture* and its *easy synthetic* availability, it seemed interesting to confirm the preceding results and to extend the scope of the system through structural modification. The incorporation of one or several methylene groups into the benzylic position was thus considered, for the purposes of fine-tuning the singlet excited state binding properties and to assist further investigation of the cooperativity effect. The coronands TTO_5O_5, XBO_5O_5 and XXO_5O_5 (Figure 2) were therefore designed. We also prepared the diphenyl analogue of BBO_5O_5 [termed $(DP)_2O_5O_5$] since it was anticipated that the more extended aromatic system would act as a better insulator between the two encapsulated metal cations (Figure 3). Finally, a related acyclic monotopic receptor (podand), TTO_5 was investigated as a reference system (Figure 4).

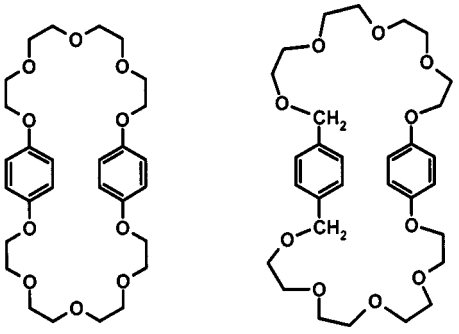

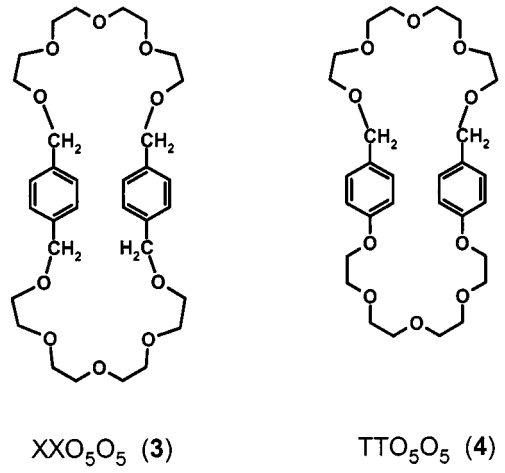

Figure 2. Bis(*p*-phenylene)coronands incorporating ten oxygen atoms, with two (**2**, **4**) or four (**3**) benzylic methylene groups; T denotes tolyl, and X xylyl

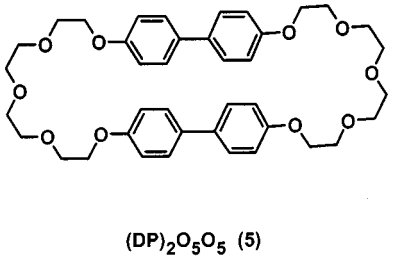

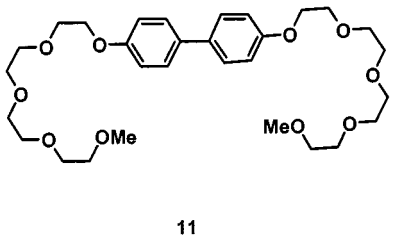

Figure 3. Bis(*p*-diphenylene)coronand **5** and its reference monochromophoric compound **11**

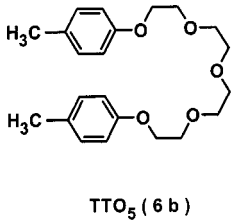

Figure 4. Acyclic monotopic receptor (podand)

As for BBO_5O_5,[3] initial screening studies showed that barium salts produced the strongest spectroscopic effects,[4b] and so Ba^{++} was selected for a systematic study of all the systems. This research is of additional interest because the coordination chemistry of Ba^{++} with organic ligands is currently under investigation in advanced materials technology.[8]

We report here the synthesis of TTO_5O_5, XXO_5O_5, XBO_5O_5, TTO_5 and $(DP)_2O_5O_5$, together with a spectroscopic study of the ligands at ambient temperature, the X-ray structure of the Ba^{++} complex of TTO_5, the determination of the association constants in the ground and excited S_1 states, a discussion of the cooperativity effect and the results of some semiempirical calculations.

2. Results and Discussion

2.1 Synthesis

As described in a preceding paper[3] on the preparation of BBO_5O_5, we employed a two-step procedure, using the

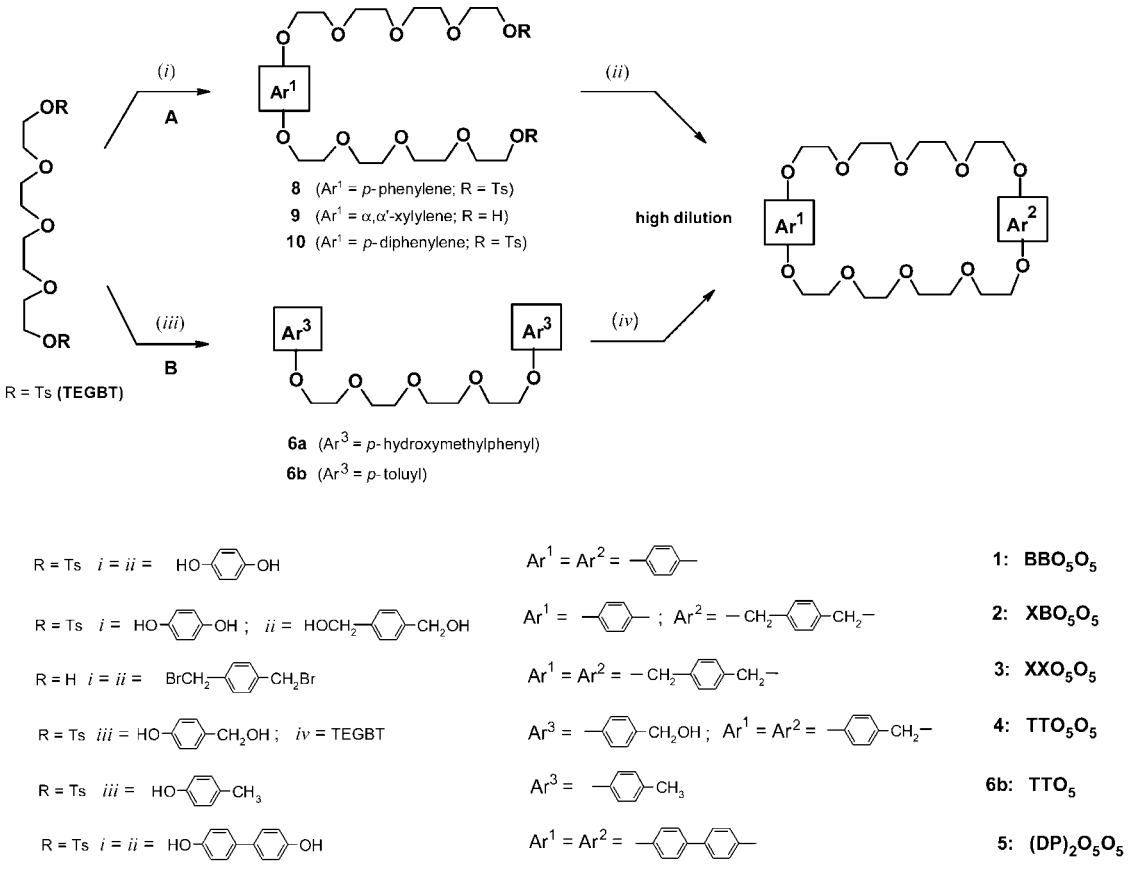

Scheme 1. Synthesis of bis(phenylene)- and bis(diphenylene)coronands by Route A (for **1**, **2**, **3** and **5**) or B (for **4** and **6b**)

high-dilution technique in the second step. Route A (Scheme 1) was followed to obtain coronands **1**, **2**, **3** and **5**, through the so-called "crab" intermediates. It does not require any functional group protection and offers the advantage of the option to select a different chromophore ($Ar_2 \neq Ar_1$) in the second step. TTO_5O_5 (**4**) and TTO_5 (**6b**) were synthesized by Route B. XBO_5O_5 (**2**) and XXO_5O_5 (**3**) have been prepared previously by other workers, by different strategies.[9] $(DP)_2O_5O_5$ has also been described, in an investigation of its mesogenic properties.[10] Most derivatives were obtained in quantities ranging from 150 to 600 mg, whilst TTO_5 was isolated in multigram amounts. The overall yields have not been optimised (see Exp. Sect.).

The structures were determined by the usual spectroscopic techniques. Only the barium complex of TTO_5 gave crystals suitable for an X-ray structure analysis, described in section 2.2.2.2.

2.2 Spectroscopic Properties

2.2.1 Coronands and Podands in the Absence of Metal Cations (Free Ligands)

2.2.1.1. Absorption Spectra

Like the *p*-disubstituted benzene derivatives,[11] compounds **1**−**4** have two important bands with maxima around 217−227 nm and 262−292 nm. In this work, we were primarily interested in the longest wavelength absorption, in order to study the effect of metal cations; typical spectra of BBO_5O_5, XBO_5O_5, TTO_5O_5 and XXO_5O_5 are given in Figure 5. Wavelength maxima and molar absorption coefficients are listed in Table 1.

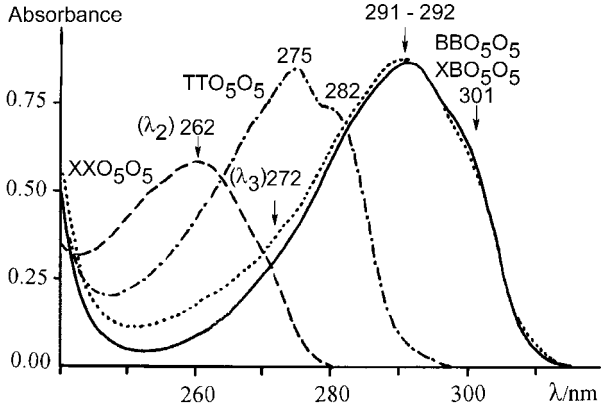

Figure 5. UV absorption spectra of **1**, **2**, **3** and **4** in acetonitrile at ambient temperature (conc. 10^{-4} M) in the 240−320 nm range; the λ_{max} values clearly indicate whether the chromophores bear two or one or no phenolic oxygen atoms; for more quantitative details, see Table 1; the spectrum of **6b** shows similar features

The spectrum of $(DP)_2O_5O_5$ is represented in Figure 6, together with that of the monochromophoric reference

Table 1. UV absorption spectra maximum wavelengths (λ_{max}) and molar absorption coefficients (ε_{max}) of the ligands **1**, **2**, **3**, **4**, **5** and **6b** in the absence and in the presence of an excess of $Ba(ClO_4)_2$ in acetonitrile; the hypsochromic shift $\Delta\tilde{\nu}$ is the difference in wavenumber between $\tilde{\nu}_{2,max}$ in the presence and in the absence of salt (λ_3 corresponds to a shoulder)

		λ_1 [nm] (ε_1 [M^{-1} cm^{-1}])	λ_2 [nm] (ε_2 [M^{-1} cm^{-1}])	(λ_3 [nm])	$\Delta\tilde{\nu}$ [cm^{-1}]
1	BBO_5O_5	227 (19015)	291 (3275)	(301)	
	BBO_5O_5 + Ba^{++}	225 (18645)	286 (4635)		600
2	XBO_5O_5	222 (16025)	291 (2925)	(301)	
	XBO_5O_5 +Ba^{++}	220 (16455)	288 (2720)		360
3	XXO_5O_5	217 (17600)	262 (570)	(272)	
	XXO_5O_5 +Ba^{++}	217 (16985)	262 (490)		0
4	TTO_5O_5	226 (23710)	275 (3490)	(282)	
	TTO_5O_5 +Ba^{++}	223 (22155)	272 (3055)	(280)	400
5	$(DP)_2O_5O_5$	201 (91960)	266 (44060)	(285)	
	$(DP)_2O_5O_5$ +Ba^{++}	201 (91960)	260 (44050)	0	865
6b	TTO_5	224 (17850)	279 (3515)	(285)	
	TTO_5 +Ba^{++}	221 (16210)	275 (2840)		520

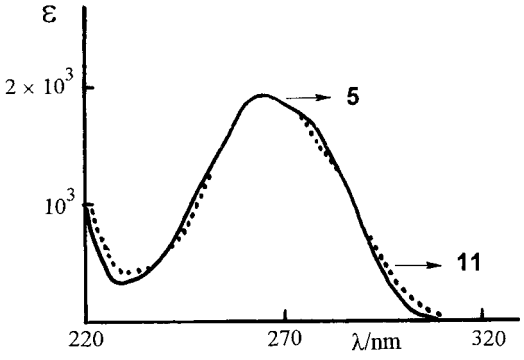

Figure 6. UV absorption spectra of **5** (—) and **11** (···) (2ε) in acetonitrile at ambient temperature

compound **11**. The spectra are very similar, implying virtually no interaction between the two diphenyl groups in **5**.

2.2.1.2. Steady-State and Dynamic Fluorescence Spectroscopy

The fluorescence spectra are represented in Figure 7 for the benzenophanes and in Figure 8 for the diphenylophane **5**. They present the same features as the reference *p*-disubstituted benzene (*p*-xylene, *p*-methylanisole and *p*-dimethoxybenzene) or diphenyl (*p*-dimethoxydiphenyl) derivatives shown in Berlman's book.[12]

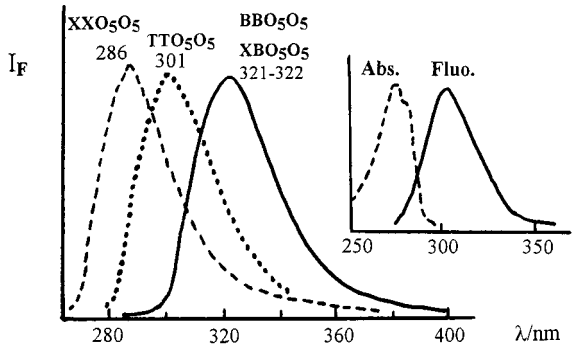

Figure 7. Fluorescence spectra of **1**, **2**, **3** and **4** in acetonitrile at ambient temperature; the spectrum of **6b** shows similar features; as shown in the inset for TTO_5O_5, they are "mirror images" of the absorption spectra (λ_{exc} see Table 2)

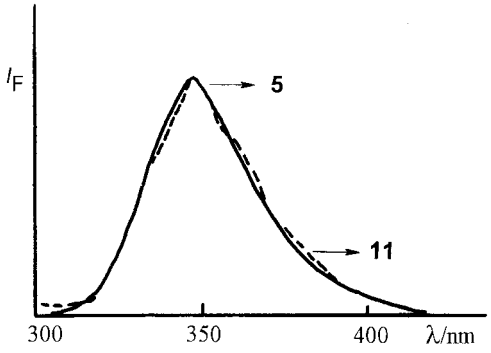

Figure 8. Fluorescence spectra of **5** and **11** in acetonitrile (normalized) at ambient temperature (λ_{exc} = 270 nm)

It should be noted that, although the UV spectra of XBO_5O_5 and BBO_5O_5 are different in the 250−290 nm range (Figure 5), the fluorescence spectra are quasisuperimposable, as shown in Figure 7. This is the result of an energy transfer between the *p*-xylyl chromophore and the hydroquinol diether chromophore, as demonstrated by Ballardini et al.,[9] who observed only the 1,4-dimethoxybenzene subunit fluorescence spectrum, regardless of the excitation wavelength.

The onset absorption wavelengths (which appear as shoulders in the spectra, Figure 5) are similar to those of the corresponding reference molecules in cyclohexane.[11] The Stokes shifts, listed in Table 2, were determined as indicators of changes of geometry in the S_1 state.

It may be noted that the shift is normal for *p*-xylene and XXO_5O_5 (ca. 1600 cm^{-1}), but increases for *p*-methylanisole (1850 cm^{-1}) and TTO_5O_5 (2350 cm^{-1}) as well as for *p*-dimethoxybenzene (3000 cm^{-1}) and BBO_5O_5 (2050 cm^{-1}). For *p*-dimethoxydiphenyl and $(DP)_2O_5O_5$, the Stokes shifts are raised to ca. 6000 cm^{-1}, which suggests a large change of geometry in the chromophore in the S_1 state. Table 2 also lists the fluorescence quantum yields, which were found to be a little lower than those of the corresponding reference molecules (except for XXO_5O_5, which is seen to experience

Table 2. Steady-state and kinetic parameters of the fluorescence of compounds **1**, **2**, **3**, **4**, **5** and **6b** in the absence and in the presence of Ba^{++} in acetonitrile, at ambient temperature; the Stokes shifts of these free ligands (fluorescence absorption) compare well with those of the reference monochromophores

		λ_{exc} [nm]	λ_{max} [nm]	Stokes shift [cm^{-1}]	Φ_F [a]	$\Delta\tilde{\nu}_{max}$ [cm^{-1}] with excess Ba^{++}	Kinetic parameters A	$1/\lambda$ [ns]
1	BBO_5O_5	280	322	2070	0.18	–	0.70	0.8
							0.80	3.7_5
	BBO_5O_5 + Ba^{++}	280	320	–	0.05	195	1.40	0.8
							0.05	5.5
2	XBO_5O_5	290	321	2070	0.15[b]	–	0.08	2.7[b]
	XBO_5O_5 + Ba^{++}	290	319	–	0.03	196	1.92	0.5
							0.20	1.9
3	XXO_5O_5	260	286	1600	0.06	–	0.27	3.0
							0.60	22.0
	XXO_5O_5 + Ba^{++}	260	286	–	0.02	0	0.09	4.3
							0.67	15.6
4	TTO_5O_5	274	301	2350	0.22	–	0.66	6.1
	TTO_5O_5 + Ba^{++}	274	298	–	0.05	335	0.94	1.4
							0.32	3.3
5	$(DP)_2O_5O_5$	270	346	6000	0.16	–	0.82	12.1
	$(DP)_2O_5O_5$ + Ba^{++}	270	343	–	0.04	252	0.60	2.9_5
							0.20	5.2_5
6b	TTO_5	279	304		0.26	–	0.72	6.8
	TTO_5 + Ba^{++}	279	302	–	0.09	218	0.40	4.3

[a] All solutions were studied under freeze and thaw degassed conditions. The fluorescence decays were recorded at λ_{max}. [b] Ballardini et al.,[9] found $\Phi_F = 0.09$ and $\tau_F = 2.2$ ns using aerated samples.

strong quenching if these data are compared with those of *p*-xylene ($\Phi = 0.40$, $\tau_F = 40$ ns) in cyclohexane.[12]

2.2.1.3. Transient Kinetic Analysis

Considering Table 2, it may be observed that most fluorescence decay times ($1/\lambda$ parameters) were found to be less than 10 ns, except for XXO_5O_5 and $(DP)_2O_5O_5$. The interpretation of the results regarding TTO_5 seems straightforward; the observed single exponential decays correspond to the lifetimes of the free ligand and of the barium complex, respectively, with the second being shorter, in keeping with a lower quantum yield. The decays of XBO_5O_5, TTO_5O_5 and $(DP)_2O_5O_5$ (free ligands) could be fitted by single exponentials, indicating no intramolecular bichromophoric interactions on the nanosecond timescale. Such interactions were, however, found to occur for BBO_5O_5 and XXO_5O_5 (which undergo biexponential decays), but they did not produce excimer-type emission in the steady state spectra as reported by previous authors for benzene[13] and diphenyl[14] derivatives.

2.2.2 Coronands and Podands in the Presence of Metal Cations

2.2.2.1. General Observations

As expected from previous results in which phenolic oxygen atoms were found to participate in the complexation of metal cations,[3,7] a *hypsochromic shift* was observed in the UV absorption spectra of **1**, **2**, **4**, **5** and **6b** in acetonitrile on addition of salts. This effect was not detected for **3**, devoid of phenolic oxygen atoms. A screening of the alkaline and alkaline earth perchlorate effects showed that Ba^{++} gave the strongest shifts (see Figure 9). This study therefore refers only to Ba^{++} complexation. As for absorption, Ba^{++} was found to have the strongest influence on fluorescence spectra, essentially through quenching of emission intensities (see Figure 10).

These spectroscopic changes are associated with metal cation complexation by the coronands **1**–**5** and the podand **6b**. All attempts to grow single crystals from **1**–**5** and Ba^{++}

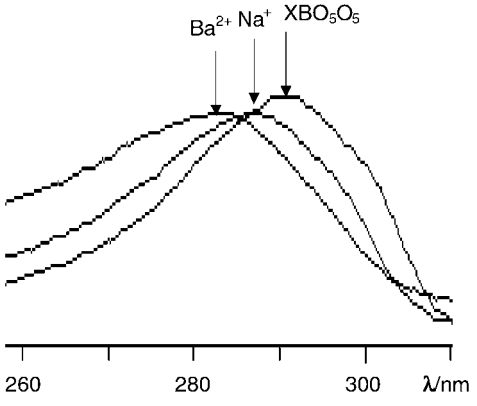

Figure 9. Influence of some alkali and alkaline earth cations on the UV spectra of XBO_5O_5

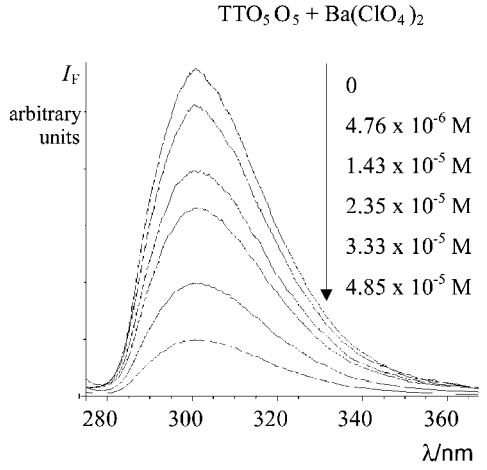

Figure 10. Influence of gradual addition of $Ba(ClO_4)_2$ on the fluorescence intensity of TTO_5O_5 (conc. 1.95×10^{-5} M); $\lambda_{exc} = 265$ nm (isosbestic point)

failed. However, crystals suitable for X-ray structure analysis were obtained for $Ba^{++} \subset TTO_5$.

2.2.2.2 X-ray Crystal Structure Analysis of TTO_5Ba^{++}

Prismatic, colourless crystals suitable for structure analysis were grown by slow evaporation of a solution composed of a mixture of dichloromethane and *n*-pentane at ambient temperature. Two projections of a single, crystallographically independent 1:1 complex are shown in Figure 11.

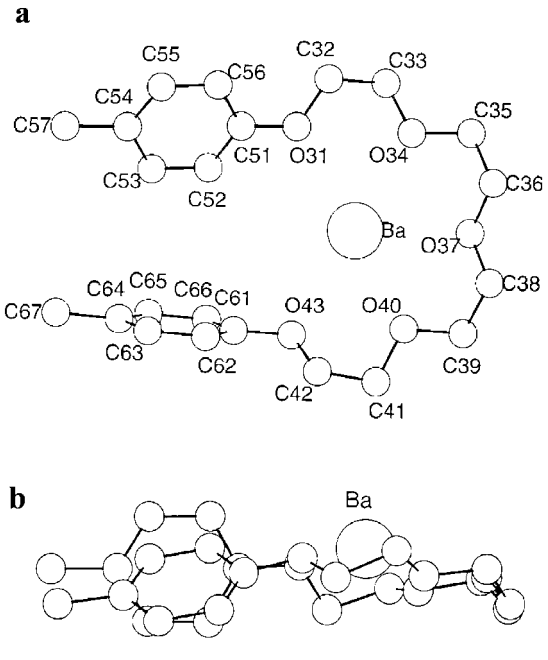

Figure 11. Projections of a crystallographically independent 1:1 complex (TTO_5Ba^{++}): **a**: on the five oxygen atoms of the polyethyleneoxy ring mean plane, along with the atomic labelling; **b**: perpendicularly to this plane; the Ba^{++} cation lies at 0.496(5) Å above the polyethyleneoxy mean plane

Table 3. Selected torsion angles [°] and their standard deviations

C32−O31−C51−C52	171.2(5)	C36−O37−C38−C39	177.6(5)
C51−O31−C32−C33	−173.9(4)	O37−C38−C39−O40	−63.7(4)
O31−C32−C33−O34	−63.9(4)	C38−C39−O40−C41	−157.0(5)
C32−C33−O34−C35	−162.4(4)	C39−O40−C41−C42	171.5(5)
C33−O34−C35−C36	173.4(5)	O40−C41−C42−O43	64.5(4)
O34−C35−C36−O37	61.9(4)	C41−C42−O43−C61	166.7(4)
C35−C36−O37−C38	−179.6(5)		

The conformation of the TTO_5 molecule is entirely defined by the torsion angles given in Table 3. Both toluene groups point in the same direction but are not parallel; the dihedral angle is close to 65°. The projection of the structure on the (*x*0*z*) plane has alternate sheets of the cation complexes on one side and the ClO_4^- anions on the other. The interactions are almost exclusively of the ionic type.

A selection of bond lengths is listed in Table 4. They do not show anomalous features. Of particular interest are the O···Ba^{++} distances. The cation is "wrapped up" by the polyethylenoxy chain in a hexagonal fashion [O···Ba^{++} distances between 2.785(4) and 2.955(4) Å; O···Ba^{++}···O angles close to 60°]. Five oxygen atoms belonging to the two perchlorate anions are also bound to the Ba^{++} cation with distances of between 2.824(5) and 3.030(5) Å (see Figure 12), so that the Ba^{++} cation is decacoordinated.

Table 4. Selection of bond lengths [Å] in the complex, including Ba···O and Cl···O distances; the bond lengths in the tolyl groups and the C−C distances in the polyethylenoxy chain are not given

Ba···O31	2.852(3)	Cl20−O21	1.428(5)
Ba···O34	2.766(4)	Cl20−O22	1.404(6)
Ba···O37	2.832(4)	Cl20−O23	1.430(5)
Ba···O40	2.785(4)	Cl20−O24	1.425(4)
Ba···O43	2.955(4)		
Ba···O14	2.824(5)	O31−C32	1.433(6)
Ba···O21	3.030(4)	O31−C51	1.387(6)
Ba···O23	2.827(5)	C33−O34	1.434(7)
Ba···O24	2.860(4)	O34−C35	1.423(7)
Ba···O13	2.911(4)	C36−O37	1.438(7)
O37−C38	1.438(7)		
Cl10···O11	1.410(6)	C39−O40	1.434(7)
Cl10···O12	1.399(6)	O40−C41	1.413(7)
Cl10···O13	1.424(5)	C42−O43	1.438(7)
Cl10···O14	1.440(5)	O43−C61	1.402(6)

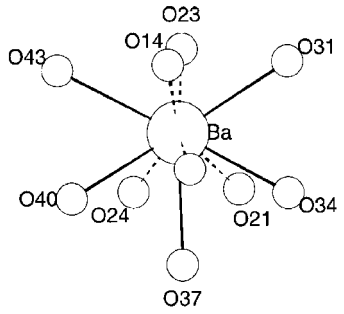

Figure 12. Coordination sphere of Ba^{++} in the crystal (O31, O34, O37, O40 and O43 belong to the podand chain and the other oxygen atoms to the perchlorate anions); for Ba^{++}···O distances see Table 4

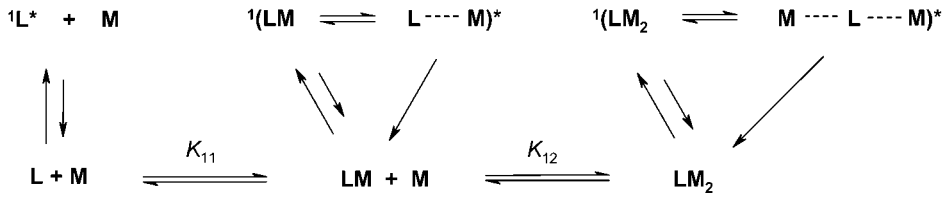

Scheme 2. Complexation of compounds **1**, **2**, **3**, **4**, **5** and **6b** by Ba^{++} (denoted L and M, respectively, for simplification); it is assumed that the interconversion between the ligand and the free cations does not occur in the S_1 state (see text)

The theoretical $Ba^{++}\cdots O$ distance is equal to 2.86 Å [$r(Ba^{++})$ = 1.35 Å and $r(O)$ = 1.51 Å]. In the structure to hand, these distances lie between 2.77 and 2.96 Å. In published structures of Ba^{++} complexes the reported Ba^{++} coordination number is usually found to be 9,[15] 10[15−17] or 11.[18]

2.2.2.3 Determination of Association Constants by Spectroscopic Methods

As shown above, the complexation of Ba^{++} by compounds **1**−**6b** clearly affects the *UV* and *fluorescence* spectra. The known LETAGROP-SPEFO method[19] was therefore used to determine the stoichiometry and the successive association constants at room temperature. The LETAGROP-SPEFO program calculates the global binding constants β for a chemical scheme (see Scheme 2, in which $\beta = K_{11}K_{21}$) by iterative comparison of calculated data with experimental data, searching for the global minimum of the error function. Equations that do not fit the data are rejected. Association constants were derived from the UV spectra ground state (see Table 5).

From transient kinetic analysis, the influence of Ba^{++} is reflected in biexponential decays (not triexponential as may have been anticipated from the existence of three kinetically distinguishable species, $^1L^*$, $^1LM_1^*$ and $^1LM_2^*$). It is likely that the complexes undergo some photodecomplexation in the relaxed singlet state, which makes the kinetic scheme difficult to establish. For deeper insight, this study would benefit from extension to other timescales and temperatures. As shown in Table 2, the fluorescence lifetimes with barium in excess are less than 5 ns (except for XXO_5O_5); the exchange of cation cannot therefore occur during the S_1 lifetime.

At low concentration (low absorbance), the fluorescence intensity is proportional to the concentration of the emitting species. Consequently, the apparent binding constants determined from the fluorescence spectra should be found to be equal, within experimental error, to those measured by UV absorption.

An example of the spectral modifications seen on gradual addition of $Ba(ClO_4)_2$ to BBO_5O_5 is presented in Figure 13, while the results of LETAGROP-SPEFO calculations are illustrated in Figure 14 for the UV spectra of $(DP)_2O_5O_5$ in the presence of increasing concentrations of $Ba(ClO_4)_2$.

All the results are collected in Table 5 and presented for comparison of the data obtained from the UV absorption and from the fluorescence spectra. In addition, experiments with $Ba(SCN)_2$ showed that a change in counteranion did not affect the fluorescence. Finally, $(n\text{Bu})_4NClO_4$ in excess was found to have no influence either on the UV or on the fluorescence spectra, since the $(n\text{Bu})_4N^+$ cation is too large to be bound to the coronands. This indicates that the ob-

Table 5. Binding constants (Scheme 2) of **1**, **2**, **3**, **4**, **5** and **6b** with $Ba(ClO_4)_2$ in acetonitrile at ambient temperature, determined from the UV absorption and fluorescence spectra, respectively, by the LETAGROP program; stoichiometries (ligand:cation) were found to be 1:1 for TTO_5, XBO_5O_5 and XXO_5O_5, and 1:1 + 2:1 for BBO_5O_5, $(DP)_2O_5O_5$ and TTO_5O_5; $\log\beta = \log K_{11} + \log K_{21}$ (β = global constant)

$Ba(ClO_4)_2$		BBO_5O_5	XBO_5O_5	XXO_5O_5	$(DP)_2O_5O_5$	TTO_5
	$\log K_{11}$[a]	3.77 ± 0.13[c]	4.08 ± 0.11	−	2.87 ± 0.08	1.99 ± 0.22
UV	$\log K_{21}$[b]	2.01 ± 0.39	−	−	2.24 ± 0.16	−
	$\log\beta$	5.78 ± 0.43	−	−	5.12 ± 0.07	−
	$\log K_{11}$	3.84 ± 0.12	4.00 ± 0.22	3.36 ± 0.06	2.73 ± 0.06	2.00 ± 0.11
Fluo	$\log K_{21}$	−	−	−	−	−
	$\log\beta$	−	−	−	−	−
BaX_2		TTO_5O_5 (X = ClO_4)	TTO_5O_5 (X = SCN)			
	$\log K_{11}$	4.75 ± 0.68				
UV	$\log K_{21}$	5.51 ± 1.29				
	$\log\beta$	10.26 ± 0.612				
	$\log K_{11}$	4.45 ± 0.01	4.48 ± 0.18			
Fluo	$\log K_{21}$	4.66 ± 0.13	4.64 ± 0.30			
	$\log\beta$	9.11 ± 0.12	9.12 ± 0.07			

[a] "log" denotes $\log_{10}$ (decimal logarithm). [b] $\log K_{21}$ was obtained by subtracting $\log K_{11}$ from $\log\beta$. [c] The statistical errors are ca. 3σ.

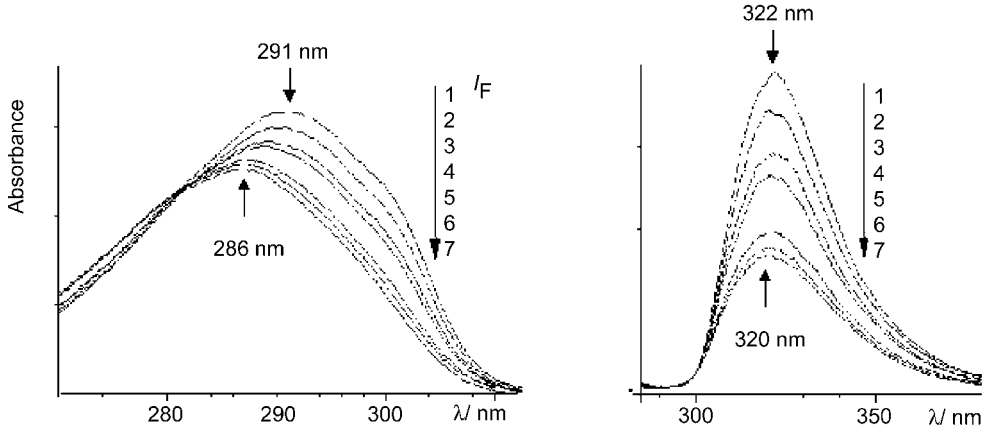

Figure 13. UV absorption and fluorescence spectra of BBO_5O_5 in acetonitrile (conc. 3.10^{-5} M) and their modification in the presence of $Ba(ClO_4)_2$; conc. [mol·L^{-1}]: **1**: 0.0; **2**: $5\cdot10^{-5}$; **3**: $1\cdot10^{-4}$; **4**: $2\cdot10^{-4}$; **5**: $5\cdot10^{-4}$; **6**: $8\cdot10^{-4}$; **7**: $1\cdot10^{-3}$; λ_{exc} = 280 nm (isosbestic point)

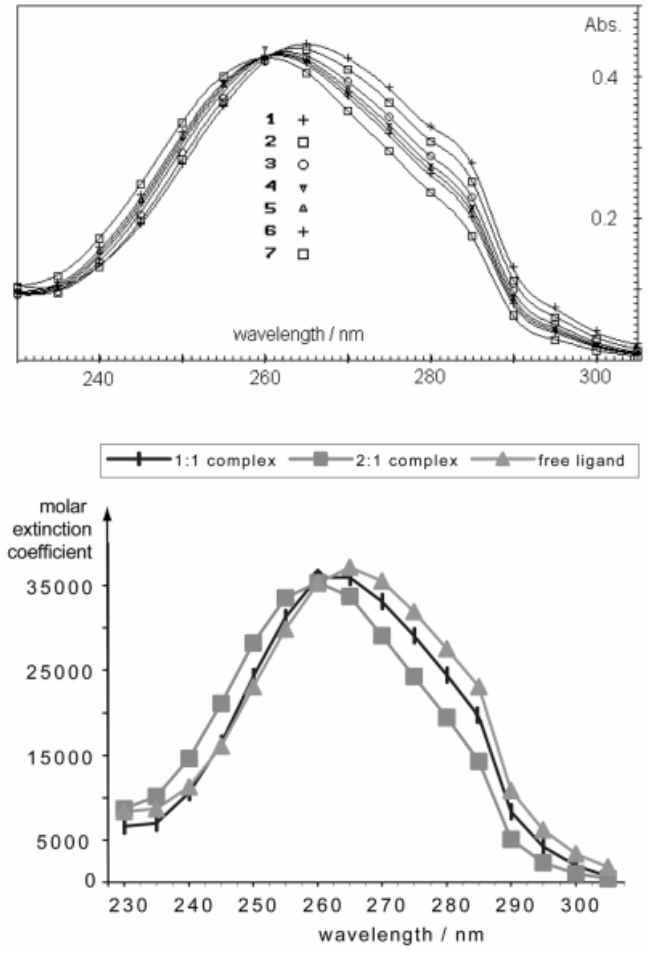

Figure 14. Top: LETAGROP plot for the determination of the stoichiometry and association constants of $(DP)_2O_5O_5$ with $Ba(ClO_4)_2$ in CH_3CN, from UV titration results between 230 and 305 nm (16 wavelengths and seven different salt concentrations (−− simulated spectra); bottom: UV spectra of the 1:1 and 2:1 complexes (calculated) and of the free ligand

served spectral alterations should not be attributed merely to ion-pair effects, but essentially to metal cation complexation.

Stoichiometries

A 1:1 (ligand/cation) stoichiometry was assigned to XBO_5O_5, XXO_5O_5 and TTO_5. The other ligands − BBO_5O_5, TTO_5O_5 and $(DP)_2O_5O_5$ − were found to display both 1:1 and 2:1 stoichiometries (Table 5), at least in the ground state. That a 2:1 stoichiometry is likely has been demonstrated by single-crystal X-ray structure analysis of the closely related 2 $Sr^{++} \subset BBO_5O_5$ complex.[3a]

Magnitude of the Binding Constants

The order of magnitude of the binding constants of Ba^{++} in coronands was found by previous authors to be diverse (log K = 1.7−7.7), essentially depending upon the structure of the monotopic receptor and the nature of the solvent;[20a−20c] they seem only rarely to have been measured in acetonitrile. Typical data for the 1:1 complexes with benzeno15-crown-5 (B15C5),[21] C_{153}-crown(O_4)[22] and CDS-crown(O_4)[23] are mentioned below.

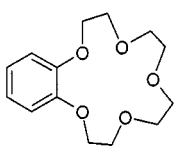

B15C5
log K : 2.60
(NMR)

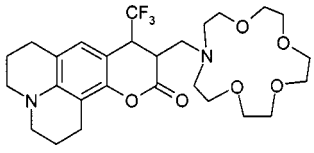

C_{153}-crown(O_4)
log K : 6.7
(spectroscopy)

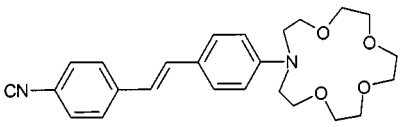

CDS-crown(O_4)
log K: 3.7
(spectroscopy)

None of these molecules closely resemble the compounds under study (Table 5). Those that exhibit a 1:1 stoichiometry have log K = 2.0 (TTO_5), 3.35 (XXO_5O_5) or 4.0 (XBO_5O_5). The latter constants were expected to be larger, because XXO_5O_5 and XBO_5O_5 are coronands whereas the first value is that of a podand. The macrocyclic effect on the increase in the association constant is not as large as that observed in simpler systems.[17] The binding constant of XXO_5O_5 could not be determined by UV in the ground state because the metal cations have no influence on the spectrum (no phenolic oxygen atom). The absence of 2:1 complexes in the above cases suggests that these complexes would be too highly strained.

Partial Photodecomplexation

It is noteworthy that the hypsochromic shifts observed in the fluorescence spectra (see $\Delta\tilde{\nu}$; Table 2) are lower than those found in the UV spectra (see $\Delta\tilde{\nu}$; Table 1; see also Figure 13). The hypsochromic shift ($\Delta\tilde{\nu} > 0$) is attributable to a decrease in conjugation between the phenolic oxygen lone pairs and the aromatic rings, due to coordination to the metal cation. This shift is expected to decrease in the singlet excited state because the charge density on the oxygen atoms becomes lower; this is known to be behind the increased acidity of phenols in the singlet excited state[24] (see next section).

This phenomenon would give rise to ionic repulsion between M^{++} and the relatively "positive" phenolic oxygen atoms, decreasing the coordination strength between the phenolic oxygen atoms and the guest cations. An additional factor in such a weaker contact may be a change in the geometry of the receptor (see Section 2.4.). As a consequence, the complexes $^1(LM)^*$ and $^1(LM_2)^*$ in the relaxed S_1 state tend to resemble the free ligand $^1L^*$ (Scheme 2) and so increase its apparent relative concentration. The binding constants determined from the fluorescence data may therefore appear lower. This is indeed the case for BBO_5O_5, $(DP)_2O_5O_5$ and, to a lesser extent, for TTO_5O_5. It should be emphasised that, in the absence of compelling structural evidence and ab initio calculations, these explanations remain tentative.

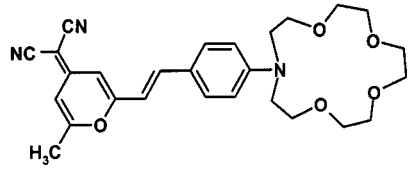

DMC-crown(O_4)

Similar observations have been made by other workers on 1:1 complexes of *azacrown ether derivatives* [DMC-crown(O_4) with Ca^{++}][4] and evidence of the release of metal cations was provided by steady-state and ultra-fast spectroscopy.[4,5] Other authors have also claimed such a photodisplacement for a benzocrown ether, termed *photoinduced recoordination of the metal cation.*[7] All these examples refer to internal charge transfer transitions in dissymmetrical compounds, in contrast with our symmetrical systems.

2.3. Cooperativity

One of the major issues in supramolecular chemistry is *cooperativity*, a property of self-organised systems.[1] The phenomenon is well documented both in biotic[25−26] and in abiotic systems.[26−28] Metal cation complexation of *ditopic receptors* is a simple case; the two binding constants K_{11} and K_{21} (Scheme 2) are compared to one another. It has been demonstrated[27] that, under statistical factors (i.e., when a system obeys this equation, the second receptor behaves independently of the first one) the result is: $K_{21} = K_{11}/4$; this is referred to as *non*cooperativity. When $K_{21} < K_{11}/4$, the cooperativity is said to be *negative*, while $K_{21} > K_{11}/4$ indicates a *positive* cooperativity; the first step then makes the second step easier. Many examples can be found in the literature.[28]

As shown in Table 5, the ditopic systems of this study, which give 1:1 and 2:1 complexes, display (*within experimental error*) three situations.

a) $(DP)_2O_5O_5$ shows virtual *non*cooperativity in the ground state, presumably because, as intimated in the introduction, the large degree of π-electron shielding prevents ionic repulsion between the cations.

b) BBO_5O_5 experiences *negative* cooperativity in the ground state; it seems that the second cavity, generated by the first encapsulation, offers an unfavourable geometry for complexation and the 2:1 complex may have no compensation for ionic repulsion.

c) TTO_5O_5 displays *positive* cooperativity and much higher values of the binding constants, which appear *remarkable* for such a coronand. This may be the result of a favourable geometry in the 2:1 complex, in which one of the pseudo crown ether moieties has more basic coordinating sites (oxygen atoms linked to the CH_2 groups). For such strong complexes, the cooperativity is maintained in the excited state.

This contrast between negative and positive cooperativity with the same guest but with a slight structural modification in the host is illustrated in the computed distribution diagrams (Figure 15).

2.4. Theoretical Studies

2.4.1. Results

The results in Table 5 point, for some ditopic receptors, to a less efficient binding ability in the excited singlet state than in the ground state. The discrepancy is striking for BBO_5O_5 and $(DP)_2O_5O_5$, which, according to our analysis, form 2:1 complexes in the ground state and only 1:1 complexes in the fluorescent state. A tentative explanation based on electronic and geometric factors has been proposed previously. As an approach towards substantiating those proposals, semiempirical calculations (AM1) were performed (see Exp. Sect.) on the *reference* chromophores − *1,4-dimethoxybenzene* (DMB) and *4,4′-dimethoxydiphenyl* (DMDP) − considered as *isolated* molecules. Previously published

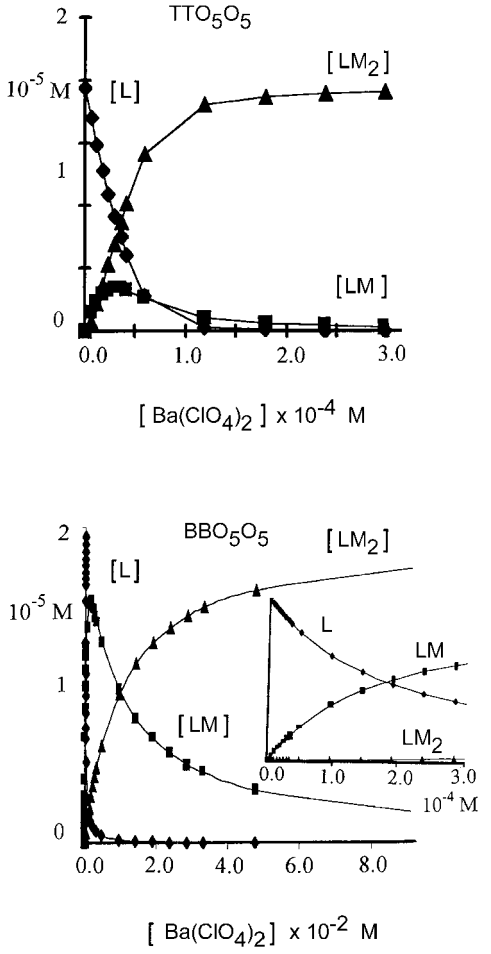

Figure 15. Computed % distribution diagrams[19] of TTO_5O_5 and BBO_5O_5 (conc. 10^{-4} M) as the Ba^{++} concentration increases; for TTO_5O_5, the 2:1 complex largely dominates at $[Ba^{++}] \approx 10^{-4}$ M (positive cooperativity), whereas for BBO_5O_5 at $[Ba^{++}] \leq 10^{-2}$ M the 1:1 complex prevails (negative cooperativity); the inset shows the early stages of BBO_5O_5 in the presence of small Ba^{++} concs. ($\leq 3 \cdot 10^{-4}$ M), for comparison with TTO_5O_5; please note the change of scale between the diagrams for TTO_5O_5 and for BBO_5O_5

work on theoretical studies of these two compounds either did not address the same question or focussed its analysis on the π-electron system alone.[29]

1,4-Dimethoxybenzene (DMB)

The molecule is represented in Figure 16; the long in-plane axis (through the OCH_3 substituents) was directed along *x* and the short in-plane axis was directed along *y*; the computation took four molecular orbitals (HOMO−1, HOMO, LUMO, LUMO+1; denoted −2, −1, +1, +2, respectively) into account.

It is noteworthy that the coefficients on the substituted carbon atoms are nonzero in both the frontier orbitals; this points to the electronic influence of the substituents on the HOMO−LUMO transition. As a result of the computation, four electronic transitions were found (see Table 6).

Table 6. Computed electronic transitions for DMB

	λ_{max} [nm]	Polarization	Status
−1 + 2	347	*y*	forbidden
−1 + 1	279	*x*	weak
−2 + 2	214	*x*	strong
−2 + 1	205	*y*	strong

The transitions at 279 and 214−205 nm correspond fairly well to the experimental observations for BBO_5O_5 [λ_{max} = 291 nm (weak) and 226 nm (strong), respectively] in acetonitrile. The net charges in Figure 17 indicate a migration of electronic density, through electronic excitation, from both juxtanuclear oxygen atoms towards the benzene ring. The optimised geometries of the ground state and of the excited state imply a large variation in the dihedral angle between the plane containing $(CH_3)_1-O-C_{Ar}$ and the benzene ring coplanar with the second OCH_3.

4,4′-Dimethoxydiphenyl (DMDP)

Because of the presence of two benzene rings linked with each other, the number of molecular orbitals involved in

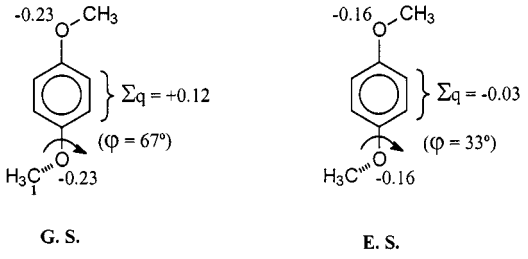

Figure 17. Net charges on the oxygen atoms and on the benzene ring (C_6H_4) in the ground state (G.S.) and in the fluorescent state (E.S.); the results indicate an increase in the electronic density in the ring from G.S. to E.S., at the expense of both phenolic oxygen atoms; "φ" denotes the dihedral angle between the plane including $(CH_3)_1-O-C_{Ar}$ and the benzene ring coplanar to the second OCH_3

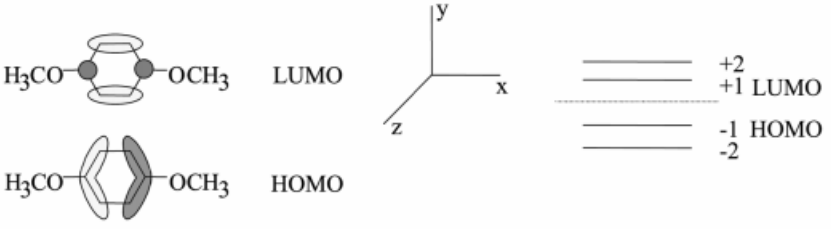

Figure 16. Left: highest occupied (HO) and lowest unoccupied (LU) molecular orbitals (MO) of DMB, calculated by the AM1 method; the HOMO−LUMO transition is polarized essentially along the *x* axis; right: molecular orbitals considered for the calculation

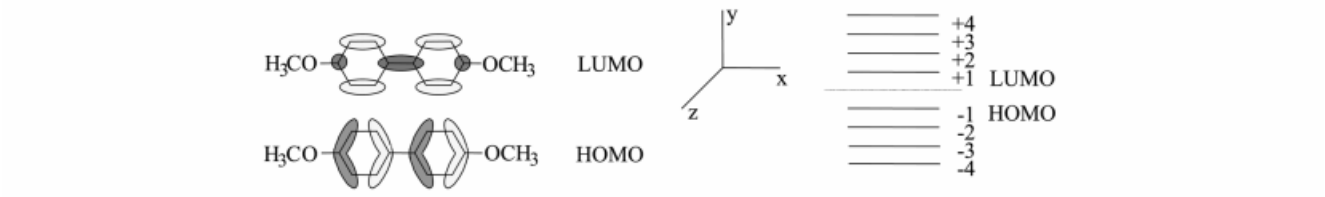

Figure 18. Left: highest occupied (HO) and lowest unoccupied (LU) molecular orbitals (MO) of DMBP calculated by the AM1 method; the HOMO−LUMO transition is polarized along the *x* axis; right: molecular orbitals considered for the calculation

the calculation should be twice that used for DMB. They were denoted −4 to +4 (Figure 18). The computed electronic transitions are described in Table 7.

Table 7. Computed electronic transitions for DMDP

	λ_{max} [nm]	Polarization	Status
−1 + 2	270	*x*, *y*	forbidden
−1 + 3	270	*z*	forbidden
−1 + 1	265	*x*	strong
−1 + 4	239		forbidden
−2 + 1	216	*y*	forbidden
−1 + 3	198	*y*	very weak
−3 + 2	197	*x*	strong
−4 + 3			

The allowed transitions [−1 + 1 and (−3 + 2) + (−4 + 3)] correspond well to those observed for DMDP or $(DP)_2O_5O_5$ ($\lambda_{max} \approx 265$ and 200 nm, respectively) in acetonitrile. Other data of interest such as the charge density on the oxygen atoms and the dihedral angle ω between the two benzene rings are displayed in Figure 19.

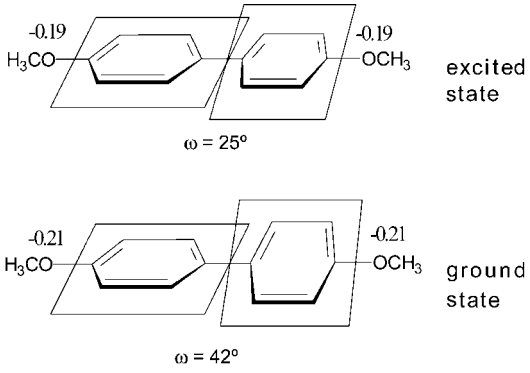

Figure 19. Net charge on the oxygen atoms in the ground state and in the fluorescent state of DMDP; they point to a decrease in electronic density in the excited state; ω is the dihedral angle between the benzene rings, which tend to be more conjugated in the excited state

2.4.2. Discussion

Although the calculations are crude in comparison with the complexity of the systems studied, the results confirm our expectations.

For DMB, the charge density on the oxygen atoms experiences a clear decrease in the excited state, whereas the dihedral angle (see Figure 17) experiences an angle change (Δ ≈ 34°). It is likely that similar changes also affect BBO_5O_5, which may explain the observed decrease in the association constant in the excited state (Table 5); the barium cations should be repelled by electron-deficient phenolic oxygen atoms and, in addition, the benzene rings might repel each other, making the second complexation more difficult.

In the case of DMDP, the difference in charge on the oxygen atoms is not as large as for DMB but the dihedral angle variation seems significant. It suggests that for $(DP)_2O_5O_5$ the increase in coplanarity might give rise to unfavourable geometric factors and also increase the cation−cation repulsion in the excited state.

3. Conclusions

It has been shown that a *family of flexible ditopic macrocyclic receptors* (benzeno- and diphenylophanes) displays a gamut of binding abilities for the *barium cation*, as well as of forms of cooperative behaviour, in acetonitrile. One of these, TTO_5O_5, exhibits strong association constants (log $K_{11} \approx 4.75$, log $K_{21} \approx 5.50$) and positive cooperativity. These systems may be considered as new ligands for the barium cation.

The binding ability seems to decrease in the fluorescent state, especially for BBO_5O_5 and $(DP)_2O_5O_5$. These results, unexpected for *symmetrical* systems, may be attributable to a decrease in the charge on the phenolic oxygen atoms and a change of geometry in the excited state. Further investigations geared towards structural determination and a deeper understanding of the mechanism are in progress.

4. Experimental Section

General: Column chromatography was performed on silica gel (SDS, chromagel Silice 60 A C.C). NMR spectra were recorded with Bruker AC 250 and WP-200SY spectrometers (250 and 200 MHz for ^{1}H, respectively, and 62 and 50.3 MHz for ^{13}C, respectively). UV/Vis spectra were recorded with a Hitachi U-3300 spectrophotometer. Emission spectra were recorded with a Hitachi F-4500 fluorescence spectrophotometer, corrected for emission and excitation. IR spectra were measured with a Fourier transform Perkin−Elmer Paragon 1000 PC spectrophotometer, as films between two KBr plates or as KBr pellets. Electron-impact mass spectra were measured with a Hewlett−Packard HP-MS 5988A. HRMS data were obtained with an Autospec EQ spectrometer.

Spectroscopic Studies: A microbalance (Mettler UM 3, sensitivity 0.1 μg) was used to weigh the samples to be dissolved in spectroscopic grade solvents for spectrophotometric measurement. No fluorescent contaminants were detected upon excitation in the wavelength region of experimental interest. The fluorescence *quantum yields* were determined by comparison with *p*-xylene in cyclohexane as the standard[12] and a refraction index correction was effected. Fluorescence *decay measurements* were performed by the single-photon timing technique as already described.[30] The samples (conc. $< 10^{-5}$ M) were degassed by freeze-pump-thaw cycles in a high-vacuum line and sealed under vacuum. The fluorescence decay, recorded at ambient temperature, was fitted by a single exponential [$i(t) \propto A \cdot \exp(-\lambda t)$] or by a sum of two exponential components [$i(t) \propto A_1 \exp(-\lambda_1 t) + A_2 \cdot \exp(-\lambda_2 t)$]. The experimental decay profiles were fitted by the Decan 1.0 program.[31] Distribution of residuals, the Durbin-Watson parameter and chi-square were used to evaluate the goodness of the fit.

Metal-Coordination Studies: Samples for UV/Vis and emission spectra were adjusted to linear-range response. Aliquots of the salt solution were added to the crown ether stock solution (2 mL), and the final volume was adjusted to 10 mL. Spectra were recorded and their intensities analysed by the LETAGROP-SPEFO program.[15] Stoichiometries and values for the equilibrium constant K were then obtained (standard deviation $\pm 3\sigma$).

Semiempirical Calculations: Because of the size of the molecular systems studied, the semiempirical AM1 approach proposed by Dewar et al.[32] was selected to calculate the fully optimized equilibrium geometries, molecular orbital pattern, charge densities and transition energies coupled with their oscillator strengths. The AMPAC 5.1 version package was used to perform the C.I. calculations, which were based on all the single and double excitations involving ten occupied and ten unoccupied molecular orbitals.

Preparations: Solvents for synthesis were dried according to standard procedures. Tetraethylene glycol, 4-hydroxybenzyl alcohol, α,α′-dibromo-*p*-xylene, 1,4-dihydroxymethylbenzene, *p*-cresol and 4,4′-biphenol were obtained from Aldrich and used without further purification. 1,11-Bis(*p*-tolylsulfonyloxy)-3,6,9-trioxaundecane (TEGBT),[33] 1,4-bis[1-(*p*-tolylsulfonyloxy)-3,6,9-trioxaundecyloxy]benzene (**8**)[3] and 1,4,7,10,13,20,23,26,29,32-decaoxa[13.13]-(1,4)-benzenophane (BBO_5O_5)[3] were prepared according to published procedures. With coronands and, especially, oily compounds, elemental analysis often gave inadequate results, and high-resolution mass spectra were therefore recorded. For the usual workup to extract and purify the products, the use of distilled water is recommended.

1,4,7,10,13,22,25,28,31,34-Decaoxa[14.14]-(1,4)-benzenophane (XBO_5O_5) (2): THF (600 mL) and NaH (8 mmol) were placed under nitrogen in a three-necked flask equipped with a condenser and a dropping funnel. The system was stirred and heated under reflux and a solution of 1,4-dihydroxymethyl benzene (0.47 g, 3.4 mmol) in THF (20 mL) was added. After 1 h, 1,4-bis[1-(*p*-tolylsulfonyloxy)-3,6,9-trioxaundecyloxy]benzene (**8**) (2.6 g, 3.4 mmol) was added dropwise to the mixture over 1 h. After refluxing for 4 d, the reaction mixture was allowed to cool to room temperature and filtered. Evaporation of the solvent and column chromatography (silica gel; ethyl acetate) of the residue afforded **2** (150 mg, 7%) as a colourless oil.[9] IR (neat): $\tilde{\nu}$ = 2919, 2870, 1510, 1455, 1352, 1289, 1232, 1109, 941, 826 cm^{-1}. ^1H NMR (250 MHz, $CDCl_3$): δ = 3.56 (m, 4 H), 3.67 (m, 20 H), 3.81 (m, 4 H), 4.04 (m, 4 H), 4.50 (s, 4 H), 6.80 (s, 4 H),7.27 (s, 4 H). ^{13}C NMR ($CDCl_3$): δ = 68.4, 69.7, 70.0, 70.9, 71.0, 71.1, 73.2, 115.9, 128.0, 137.9, 153.3. UV/Vis (acetonitrile): λ_{max} (ε) = 222 (16027), 292 nm (2926). FAB-HRMS: $C_{30}H_{44}O_{10}$ calcd. 564.2934 [M^+], found 564.2945.

2,5,8,11,14,23,26,29,32,35-Decaoxa[15.15]-(1,4)-benzenophane (XXO_5O_5) (3): NaH (6 mmol) in THF (200 mL) was placed under nitrogen in a three-necked flask equipped with a condenser and a dropping funnel. The mixture was heated at reflux and a solution of 1,4-bis(13-hydroxy-2,5,8,11-tetraoxatridecyl)benzene (**9**) (0.75 g, 1.5 mmol) and α,α′-dibromo-*p*-xylene (0.4 g, 1.5 mmol) in THF (80 mL) was added dropwise over 4 h. Refluxing was continued for 12 h and, after cooling, the reaction mixture was filtered and the solvent was removed in vacuo. Evaporation of the solvent and column chromatography (silica gel; ethyl acetate) of the residue afforded **3** (204 mg, 23%) as a colourless oil.[9] ^1H NMR (200 MHz, $CDCl_3$): δ = 3.65 (m, 32 H), 4.52 (s, 8 H),7.27 (s, 8 H). ^{13}C NMR ($CDCl_3$): δ = 68.4, 69.7, 70.0, 73.1, 127.8, 137.5. MS (70 eV, EI): *m/z* (%) = 592 (4) [M^+], 296 (24), 104 (100). UV/Vis (acetonitrile): λ_{max} (ε) = 217 (17600), 262 nm (570).

1,4,7,10,13,21,24,27,30,33-Decaoxa[13.15]-(1,4)-benzenophane (TTO_5O_5) (4): NaH (10 mmol) in degassed (with nitrogen) THF (100 mL) was heated under reflux. A solution of 1,13-bis[4-(hydroxymethyl)benzyl]-1,4,7,10,13-pentaoxatridecane (**6a**) (406 mg, 1 mmol) and TEGBT (502 mg, 1 mmol) in THF (30 mL) was then added dropwise over 5 h. Heating and stirring were continued for 4 h. After cooling, the solution was filtered and the solvent was evaporated in vacuo. Column chromatography (silica gel; ethyl acetate) of the residue afforded **4** as a colourless oil (132 mg, 24%). IR (neat): $\tilde{\nu}$ = 2919, 2866, 1613, 1514, 1352, 1301, 1247, 1103, 944, 813 cm^{-1}. ^1H NMR (250 MHz, $CDCl_3$): δ = 3.56 (m, 4 H), 3.65 (m, 20 H), 3.82 (m, 4 H), 4.05 (m, 4 H), 4.45 (s, 4 H), 6.84 (d, $^3J_{H,H}$ = 8.6 Hz, 4 H), 7.21 (d, $^3J_{H,H}$ = 8.6 Hz, 4 H). ^{13}C NMR ($CDCl_3$): δ = 67.9, 69.6, 70.0, 71.1, 71.2, 73.2, 114.9, 131.0, 158.7. UV (acetonitrile): λ_{max} (ε) = 226 (23 708), 275 nm (3490). FAB-HRMS. $C_{30}H_{45}O_{10}$ calcd. [M^+ + H] 565.3013, found 565.3043.

1,4,7,10,13,26,29,32,35,38-Decaoxa[13.13]-(4,4′)diphenylophane (5): K_2CO_3 (3.17 g, 22.95 mmol) in suspension in acetone (150 mL) was placed under nitrogen in a 500-mL three-necked, round-bottomed flask, equipped with a reflux condenser, a dropping funnel, a pressure equalizer and a magnetic stirrer, and the mixture was heated to reflux. The ditosyl intermediate **10** (1.48 g, 1.75 mmol) and biphenol (0.34 g, 1.83 mmol), dissolved in acetone (40 mL), were then added dropwise, very slowly, over 24 h. The reflux was maintained for 2 d and the medium was allowed to cool to room temperature, filtered and dried with Na_2SO_4. After solvent removal, the brownish oil residue was chromatographed through a silica gel column [eluent: ethyl acetate/dichloromethane, 1:1 (v/v)] to provide **5** (0.322 g, yield 27%) as a white powder. M.p. 180 °C (ref.[10] 193 °C). IR (KBr): $\tilde{\nu}$ = 2938, 2873, 2363, 2343, 1604, 1499, 1351, 1270, 1245, 1179, 1133, 1063, 947, 920, 826, 802, 611, 519 cm^{-1}. ^1H NMR (250 MHz, $CDCl_3$): δ =3.75 (m, 16 H), 3.9 (m, 8 H), 4.06 (m, 8 H), 6.81−6.84 (m, 8 H), 7.27−7.30 (m, 8 H). UV/Vis (acetonitrile): λ_{max} (ε) = 201 (91958), 266 nm (44061). FAB-HRMS $C_{40}H_{48}O_{10}$ calcd. [M^+] 688.32474, found 688.32570.

1,13-Bis[4-(hydroxymethyl)benzyl]-1,4,7,10,13-pentaoxatridecane (6a): 4-Hydroxybenzyl alcohol (5.0 g, 40 mmol) was dissolved in 100 mL of a methanolic NaOH (1.6 g, 40 mmol) solution at room temperature. The methanol was evaporated in vacuo and the residue was solubilized in acetonitrile. The solvent was again evaporated in vacuo in order to remove methanol completely. The resulting sodium salt and TEGBT (10 g, 20 mmol) were refluxed in acetonitrile, with vigorous stirring, for 4 h. After cooling, the solid was filtered off and the solvent was removed in vacuo. The residue

was dissolved in CH_2Cl_2 and washed with a aqueous solution of NaOH (10%), and then with pure H_2O. The organic phase was dried with Na_2SO_4 and the solvent was removed to afford **6a** (7.5 g, 93%) as a white solid. M.p. 56−60 °C. IR (KBr): $\tilde{\nu}$ = 3365, 3200, 2936, 2878, 1654, 1611, 1512, 1299, 1247, 1126, 1102, 1064, 846, 820 cm^{-1}. ^1H NMR (250 MHz, $CDCl_3$): δ = 2.10 (br. s, 2 H), 3.70 (m, 8 H), 3.82 (m, 4 H), 4.13 (m, 4 H), 4.55 (s, 4 H), 6.85 (d, $^3J_{H,H}$ = 8.3 Hz, 4 H), 7.22 (d, $^3J_{H,H}$ = 8.3 Hz, 4 H). ^{13}C NMR ($CDCl_3$): δ = 64.9, 67.5, 69.7, 70.7, 70.8, 114.7, 128.6, 133.4, 158.4. FAB-HRMS: $C_{22}H_{30}O_7$ calcd. [M + Na^+] 429.1889, found 429.1891.

1,13-Di-*p*-tolyl-1,4,7,10,13-pentaoxatridecane (TTO_5) (6b): *p*-Cresol (4.3 g, 40 mmol) was dissolved in 50 mL of a methanolic NaOH (1.6 g, 40 mmol) solution at room temperature. Methanol was evaporated in vacuo and the residue was solubilized in acetonitrile. The solvent was again evaporated in vacuo in order to remove methanol completely. The resulting sodium salt and TEGBT (10 g, 20 mmol) were refluxed in acetonitrile, with vigorous stirring, for 16 h. After cooling, the solid was filtered off and the solvent was removed in vacuo. The residue was dissolved in CH_2Cl_2 and washed with an aqueous solution of NaOH (10%), and then with pure H_2O. The organic phase was dried with Na_2SO_4 and the solvent was removed to afford **6b** as a colourless oil (7.1 g, 95%). IR (neat): $\tilde{\nu}$ =2930, 2881, 1615, 1511, 1244, 1111, 665 cm^{-1}. ^1H NMR (200 MHz, $CDCl_3$): δ = 2.26 (s, 6 H), 3.82 (m, 4 H), 3.65 (m, 8 H), 4.08 (m, 4 H), 7.50 (d, $^3J_{H,H}$ = 8.4 Hz, 4 H), 6.80 (d, $^3J_{H,H}$ = 8.4 Hz, 4 H). ^{13}C NMR ($CDCl_3$): δ = 20.4, 67.5, 69.8, 70.7, 70.8, 114.5, 129.8, 130.0, 156.6. MS (70 eV, EI): *m/z* (%) = 374 (19) [M^+], 179 (21), 135 (100), 107 (46), 91 (71). UV/Vis (acetonitrile): λ_{max} (ε) = 224 (17 849), 279 nm (3515). FAB-HRMS: $C_{22}H_{31}O_5$ calcd. [M^+ + H] 375.2171; found 375.2172.

1,4-Bis(13-hydroxy-2,5,8,11-tetraoxatridecyl)benzene (9): Acetone (150 mL) and K_2CO_3 (40 g) were placed under nitrogen in a three-necked flask, equipped with a condenser and a dropping funnel, and the system was stirred and heated under reflux. A solution of α,α′-dibromo-*p*-xylene (2.1 g, 8 mmol) and tetraethylene glycol (3.1 g, 16 mmol) in acetone (100 mL) was added dropwise over 5 h. After having been heated and stirred for 10 h, the mixture was allowed to cool to room temperature and filtered. Removal of the solvent and column chromatography (silica gel; ethyl acetate) of the residue afforded **9** as a colourless oil (2.1 g, 53%). ^1H NMR (200 MHz, $CDCl_3$): δ = 3.65 (m, 32 H), 4.54 (s, 4 H),7.28 (s, 4 H). ^{13}C NMR ($CDCl_3$): δ = 61.7, 69.3, 70.2, 70.4, 73.7, 127.8, 137.3.

4,4′-Bis[11-(*p*-tolylsulfonyloxy)-3,6,9-trioxaundecyloxy]biphenyl (10): K_2CO_3 (18.7 g, 0.14 mmol) in suspension in acetone (250 mL) was placed in a 1000-mL three-necked, round-bottomed flask equipped as for the preparation of **5**. The mixture was heated to reflux and a solution of 4,4′-biphenol (5 g, 26.85 mmol) and TEGBT (67.8 g, 0.14 mmol) in acetone (200 mL) was added dropwise over 2 h. After 2 d of refluxing, the mixture was allowed to cool to room temperature and treated as for **5**. The brownish residual oil was chromatographed on silica gel [eluent: ethyl acetate/dichloromethane, 2:3 (v/v)]. Compound **10** (2.04 g, 9% yield) was obtained as a white powder. M.p. 59−60 °C. IR (KBr): $\tilde{\nu}$ =3074, 2934, 2881, 1608, 1501, 1453, 1360, 1244, 1177, 1108, 1054, 926, 830, 784, 665, 554 cm^{-1}. ^1H NMR (250 MHz, $CDCl_3$): δ = 2.42 (s, 6 H), 3.58−3.72 (m, 20 H), 3.84−3.88 (m, 4 H), 4.12−4.16 (m, 8 H), 7.76−7.80 (m, 4 H), 6.93−6.97 (m, 4 H), 7.30−7.33 (m, 4 H), 7.43−7.46 (m, 4 H), FAB-HRMS $C_{42}H_{54}O_{14}S_2$ calcd. [M^+] 846.29550, found 846.29534.

4,4′-Bis(3,6,9-trioxadecyloxy)biphenyl (11): K_2CO_3 (4 g, 28.9 mmol), 4,4′-biphenol (0.29 g, 1.57 mmol) and acetone (40 mL) were placed in a 100-mL three-necked, round-bottomed flask, equipped with a reflux condenser, a dropping funnel, a pressure equalizer and a magnetic stirrer, under nitrogen. The mixture was then refluxed whilst stirring, and 1-iodo-3,6,9-trioxadecane (0.86 g 3.41 mmol) in acetone (15 mL) was added. After the mixture had been heated for 36 h, it was allowed to cool, filtered and dried with Na_2SO_4. After solvent evaporation, the solution left a brown oil, which was chromatographed through a silica gel column [eluent: ethyl acetate/dichloromethane, 2:3 (v/v)] to provide **11** (0.225 g, 30% yield) as a white powder. M.p. 82 °C. IR (KBr): $\tilde{\nu}$ =2905, 2865, 1601, 1501, 1452, 1357, 1269, 1242, 1181, 1111, 1065, 949, 923, 827, 609, 563, 519 cm^{-1}. ^1H NMR (250 MHz, $CDCl_3$): δ = 3.36 (s, 6 H), 3.55−3.88 (m, 20 H), 4.13−4.15 (m, 4 H), 6.94−6.97 (m, 4 H), 7.44−7.47 (m, 4 H). UV/Vis (acetonitrile): λ_{max} (ε) = 201 (50566), 266 nm (24566). FAB-HRMS: $C_{26}H_{38}O_8$ calcd. [M^+] 478.2566, found 478.2570.

X-ray Structure Analysis: The crystal setting, the cell parameters and the data collection were performed with a CAD-4 Enraf−Nonius diffractometer, equipped with a graphite monochromator for Mo-K_α radiation. The crystal data, data collection (θ−2θ) and refinement characteristics are given in Table 8; 25 reflections with θ between 14° and 17° were used for crystal setting and least-squares refinement of cell parameters. The cell absorption correction was performed by the ψ-scan technique.[34] The crystal structure was solved by direct methods, with the MITHRIL package,[35] which provided the positions of the Ba and Cl atoms. Fourier recycling gave the positions of the remaining C and O atoms. The atomic parameters were refined with the SHELX93 package[36] anisotropically for the non-hydrogen atoms (the hydrogen atoms were placed in their theoretical positions and allowed to ride the carbon atoms to which they were attached). The final *R* and *wR* factors were equal to 0.025 and 0.035, respectively, and the goodness of fit was *s* = 1.075. Crystallographic data for the structure reported in this paper have been deposited with the Cambridge Crystallographic Data Centre as supplementary publication

Table 8. Crystal data for TTO5/$Ba(ClO_4)_2$

Empirical formula	$C_{22}H_{30}O_5 \cdot Ba(ClO_4)_2$
M_r	710.7
Crystal system	monoclinic
Space group	$P2_1/c$
Z	4
a [Å]	9.603(4)
b [Å]	16.665(4)
c [Å]	17.619(8)
β [°]	98.69(2)
V [Å^3]	2787(2)
$\rho_{calcd.}$ [g·cm^{-3}]	1.694
λ (Mo-K_α) [Å]	0.7107
absorption coefficient [mm^{-1}]	1.725
Crystal dimensions [mm]	0.4 × 0.35 × 0.5
Min. transmission (%)	0.98
Max. transmission (%)	1.0
h_{min}/h_{max} [°]	0/10
k_{min}/k_{min} [°]	0/18
l_{min}/l_{min} [°]	−19/19
θ_{max} [°]	24
Reflections measured	3867
Reflections observed	2899
Parameters	463
R	0.025
wR	0.035
Goodness of fit, *s*	1.075

no. CCDC-170496. Copies of the data can be obtained free of charge on applicaton to CCDC, 12 Union Road, Cambridge CB2 1EZ, UK [Fax: (internat.) + 44-1223/336-033; E-mail: deposit@ccdc.cam.ac.uk].

Acknowledgments

We warmly thank Dr. Françoise Chardac and Pamela Mössmer (Saarbrücken, Germany) for technical assistance. E. P.-I. is indebted to the regional government of Andalucía for a postdoctoral fellowship. Financial assistance from the Région Aquitaine is gratefully acknowledged.

[1] J.-M. Lehn, *Supramolecular Chemistry. Concepts and Perspectives*, VCH Verlagsgesellschaft, Weinheim, **1995**.

[2] P. R. Ashton, D. Philip, M. V. Reddington, A. M. Z. Slawin, N. Spencer, J. F. Stoddart, D. J. Williams, *J. Chem. Soc., Chem. Commun.* **1991**, 1680−1681 and references therein.

[3] [3a] D. Marquis, H. Greiving, J.-P. Desvergne, N. Lahrahar, P. Marsau, H. Hopf, H. Bouas-Laurent, *Liebigs Ann./Recueil* **1997**, 97−106. [3b] J.-P. Desvergne, H. Bouas-Laurent, E. Perez-Inestrosa, P. Marsau, M. Cotrait, *Coord. Chem. Rev.* **1999**, *185−186*, 357−371. [3c] J.-P. Desvergne, E. Perez-Inestrosa, H. Bouas-Laurent, G. Jonusauskas, J. Oberlé, C. Rullière, "Phototunable metal cation binding ability of some monocyclic and bicyclic receptors", in *New Trends in Fluorescence Spectroscopy, Applications to Chemical and Life Sciences*" (Eds.: B. Valeur, J. C. Brochon), Springer-Verlag, Berlin, **2001**, chapter 8, pp. 157−169. [3d] Ditopic receptors for metal cations (binucleating macrocycles) see: L. F. Lindoy, *The Chemistry of Macrocyclic Ligand Complexes*, Cambridge University Press, Cambridge, **1989**, pp. 61−76, 121−127.

[4] [4a] M. Martin, P. Plaza, T. H. Meyer, F. Badaoui, J. Bourson, J. P. Lefevre, B. Valeur, *J. Phys. Chem.* **1996**, *100*, 6879−6888. [4b] For a fluorescent chemosensor for Ba^{++} ions, see: L. Prodi, F. Bolleta, N. Zaccheroni, C. I. Watt, N. J. Mooney, *Chem. Eur. J.* **1998**, *4*, 1090−1094.

[5] G. Jonusauskas, R. Lapouyade, S. Delmond, J. P. Létard, C. Rullière, *J. Chem. Phys.* **1996**, *93*, 1670−1696.

[6] [6a] K. Kimura, R. Mizutani, M. Yokoyama, R. Anakawa, G. Matsubayashi, M. Okamoto, H. Doe, *J. Am. Chem. Soc.* **1997**, *119*, 2062−2063. [6b] I. K. Lednev, T. Q. Te, R. E. Heste, J. N. Moore, *J. Chem. Phys.* **1997**, *101*, 4966−4972. [6c] I. K. Lednev, R. E. Heste, J. N. Moore, *J. Am. Chem. Soc.* **1997**, *119*, 3456−3461.

[7] [7a] S. I. Druzhinin, M. V. Rusalov, B. M. Uzhinov, M. V. Alfimov, S. P. Gromov, O. A. Fedorova, *Proc. Indian Acad. Sci. (Chem. Sci.)* **1995**, *107*, 721−727. [7b] S. P. Gromov, M. V. Alfimov, *Russ. Chem. Bull.* **1997**, *46*, 611−636. [7c] A. D. Roshal, A. V. Grigorovitch, A. O. Doroshenko, V. G. Pivovarenko, A. P. Demchenko, *J. Phys. Chem. A* **1998**, *102*, 5907−5914.

[8] [8a] L. Hubert-Pfalzgraf, H. Guillon, *Appl. Organomet. Chem.* **1998**, *12*, 221−236. [8b] W. Clegg, S. J. Coles, E. K; Cope, F. S. Mair, *Angew. Chem. Int. Ed.* **1998**, *37*, 796−798.

[9] R. Ballardini, V. Balzani, M. T. Gandolfi, R. E. Gillard, J. F. Stoddart, E. Tabellini, *Chem. Eur. J.* **1998**, *4*, 449−459. *In this paper, formula* ***15*** *was specified wrongly; it should read* ***5*** *and corresponds to* XBO_5O_5 *(formula* ***2*** *in this work).*

[10] P. R. Ashton, D. Joachimi, N. Spencer, J. F. Stoddart, C. Tschierske, A. J. P. White, D. J. Williams, K. Zab, *Angew. Chem. Int. Ed. Engl.* **1994**, *33*, 1503−1506. For mesogenic properties, see also: D. Joachimi, P. R. Ashton, C. Sauer, N. Spencer, C. Tschierske, K. Zab, *Liq. Cryst.* **1996**, *20*, 337−348.

[11] E. S. Stern, C. J. Timmons *Introduction to Electronic Absorption Spectroscopy in Organic Chemistry*, Edward Arnold, London, **1970**.

[12] I. B. Berlman, *Handbook of Fluorescence Spectra of Aromatic Molecules*, Academic Press, New York, **1971**.

[13] [13a] J. B. Birks, *Photophysics of Aromatic Molecules*, J. Wiley Interscience, London, **1970**, pp. 330−345. [13b] F. Hirayama, *J. Chem. Phys.* **1965**, *42*, 3163−3171. [13c] H. Hopf, R. Utermöhlen, P. Jones, J.-P. Desvergne, H. Bouas-Laurent, *J. Org. Chem.* **1992**, *57*, 5509−5517.

[14] K. A. Zachariasse, W. Kühnle, A. Weller, *Chem. Phys. Lett.* **1978**, *59*, 375−380.

[15] W. A. Petitt, N. C. Baenziger, *Acta Crystallogr., Sect. C* **1994**, *50*, 221−224.

[16] H. D. Inerowicz, M. A. Khan; G. Atkinson, R. L. White, *Acta Crystallogr., Sect. C* **1994**, *50*, 688−690.

[17] B. Dietrich, P. Viout, J.-M. Lehn, *Macrocyclic Chemistry*, VCH, Weinheim, **1993**.

[18] L. P. Häming, C. A. Reiss, K. Goubitz, D. Heijdenrijk, *Acta Crystallogr., Sect. C* **1990**, *46*, 462−465.

[19] L. G. Sillen, B. Warnquist, *Ark. Kemi* **1968**, *31*, 315−339 and 337−390. J. Havel, *Haltafal-Spefo program*, Mazaryle University, Brno, Moravia, Czech Republic.

[20] [20a] R. M. Izatt, J. S. Bradshaw, S. A. Nielsen, J. D. Lamb, J. J. Christensen, *Chem. Rev.* **1985**, *85*, 271−339. [20b] H. J. Buschmann, *J. Solution Chem.* **1988**, *17*, 277−295. [20c] K. S. Choi, Y. K. Shin, S. J. Kim, *Bull. Korean Chem. Soc.* **1986**, *7*, 320−327.

[21] Y. Jayathirta, V. Krishnan, *Indian J. Chem. Sect. A* **1979**, *18A*, 311−314.

[22] J. Bourson, J. Pouget, B. Valeur, *J. Phys. Chem.* **1993**, *97*, 4552−4557.

[23] J. F. Létard, R. Lapouyade, W. Rettig, *Pure Appl. Chem.* **1993**, *65*, 1705−1712.

[24] [24a] J. A. Barltrop, J. D. Coyle, *Excited States in Organic Chemistry*, John Wiley & Sons, London, **1975**, pp. 49−51. [24b] E. Van der Donckt, *Prog. React. Kinet.* **1970**, *5*, 273−299.

[25] [25a] A. L. Lehninger, *Biochemistry, the Molecular Basis of Cell Structure and Function*, Worth Publishers, New York, **1975**. [25b] D. E. Koshland, Jr., *Enzymes (3rd ed.)* **1970**, *1*, 341−396.

[26] [26a] J. Rebek, Jr., *Acc. Chem. Res.* **1984**, *17*, 258−264. [26b] A. Pfeil, J.-M. Lehn, *J. Chem. Soc., Chem. Commun.* **1992**, 838−840.

[27] [27a] K. A. Connors *Binding Constants*, John Wiley & Sons, New York, **1987**. [27b] B. Permutter-Hayman, *Acc. Chem. Res.* **1986**, *19*, 90−96.

[28] [28a] J. Rebek, T. Costello, L. Marshall, R. Wattley, R. C. Gadwood, K. Onan, *J. Am. Chem. Soc.* **1985**, *107*, 7481−7487 and references therein. [28b] P. D. Beer, J. B. Cooper, *Chem. Commun.* **1998**, 129−130.

[29] [29a] B. Uno, T. Kubota, *J. Mol. Structure (Theochem)* **1991**, *230*, 247−261. [29b] G. Grabner, S. Monti, G. Marconi, B. Mayer, C. Klein, G. Köhler, *J. Phys. Chem.* **1996**, *100*, 20068−20075.

[30] J.-P. Desvergne, A. Castellan, H. Bouas-Laurent, J.-C. Soulignac, *J. Lumin.* **1987**, *37*, 175−181.

[31] T. de Roeck, N. Boens, J. Dockx, *DECAN 1.0*, K. U. Leuven, 301 Heverlee, Belgium.

[32] M. J. S. Dewar, E. G. Zoebisch, E. F. Healy, J. J. P. Stewart, *J. Am. Chem. Soc.* **1985**, *107*, 3902−3909.

[33] [33a] J. Dale, P. O Kristiansen, *Acta Chem. Scand.* **1972**, *29*, 1471−1478. [33b] I. Stibor, O. Kocian, P. Holy, J. Zavada, *Collect. Czech. Chem. Commun.* **1987**, *52*, 2057−2060.

[34] A. C. T. North, D. C. Phillips, F. S. Matthews, *Acta Crystallogr., Sect. A* **1968**, *24*, 351−359.

[35] C. J. Gilmore, *J. Appl. Crystallogr.* **1984**, *17*, 42−46.

[36] G. M. Sheldrick, *Program for the Refinement of Crystal Structures*, Univ. Göttingen, Germany, **1993**.

[37] P. Van der Sluis, A. L. Speck, K. Timmer, H. A. Meinema, *Acta Crystallogr., Sect. C* **1990**, *46*, 1741−1743.

Received March 20, 2001
[O01128]